

See discussions, stats, and author profiles for this publication at: <https://www.researchgate.net/publication/265163947>

Dissolved Air Flotation And Potential Clarified Water Quality Based On Computational Fluid Dynamics Modelling

Conference Paper · November 2009

DOI: 10.13140/2.1.2605.2480

CITATION

1

READS

131

2 authors:



[Tony Amato](#)

Doosan Enpure Ltd

10 PUBLICATIONS 72 CITATIONS

[SEE PROFILE](#)



[Jim Wicks](#)

The Fluid Group, Oxford, UK

34 PUBLICATIONS 403 CITATIONS

[SEE PROFILE](#)

Dissolved Air Flotation And Potential Clarified Water Quality Based On Computational Fluid Dynamics Modelling

Tony Amato CEng, CEnv, CSci, MCIWEM* and Dr Jim Wicks DPhil, CPhys, MInstP**

* Technology Manager, Enpure Ltd, Enpure House, Woodgate Business Park, Kettleswood Drive, Birmingham B323DB, UK.

(E-mail: tamato@enpure.co.uk).

** Director, The Fluid Group, Magdalen Centre, The Oxford Science Park, Oxford OX44GA, UK

(E-mail: jim.wicks@thefluidgroup.com).

Abstract The purpose of this paper will be to report on the potential impact on the clarified water quality produced by a Dissolved Air Flotation (DAF) plant, designed and built on the basis of conventional rates (i.e. ~10 m/h Net, excluding recycle) and assessing when using the same structures loaded at higher rates how the product quality may change or online monitoring such as turbidity may be affected.

The assessment has been based on the use of both Computational Fluid Dynamics (CFD) and a small number of full scale site trials.

KEYWORDS Computational fluid dynamics; dissolved air flotation, loading rate, water treatment and subnatant quality.

INTRODUCTION

The application of both DAF and CFD within the water industry is regarded as well established; however the modelling of DAF presents a multiphase challenge, in that air or gas, water and solids in the form of previously coagulated and flocculated material are present. These three phases make any computer analysis particularly complex. In an attempt to simplify the approach and free up valuable computer resources this paper will report on how it is possible to assess ultimate water quality by simulating the three phases. This will be by using varying bubble size and densities within the main zones of the DAF cell under consideration. In the case of the latter variable a change in density is used to simulate an assumed collection of bubbles and particulate as single spherical agglomerates.

The primary objectives of the study and results reported were to derive an approximate predictive tool which would allow the designer to not only consider DAF loading rate as a function of flow and tank surface area but also in part relate this to the tank depth. This in turn would allow a risk assessment to be made of the likely impact on water quality in terms of turbidity that the selected loading rate and tank depth might have on the treated water leaving the DAF cell.

The basic assumption made from the start was that the "white water level" (WWL), defined here as the milky white solution that develops on release of the air from the pressurised recycle water through proprietary air release devices and subsequently establishes a stratified layer, as reported by Amato et al 2007 and 2009 and Guimet et al 2007, under the floated sludge layer that develops on the water surface within the DAF cell, will contribute to the ultimate product quality. Essentially that if the lower level approaches or is below the take off, whether using subnatant tubes, perforated floor or an exit underflow baffle then it will have an increasing likelihood of producing deteriorating water quality.

In addition and to a limited extent the impact of any rotational flow imparted to the main body of water as it passes through the flocculators and into the DAF cell will also be reported particularly its potential impact on water quality and desludging.

A number of scenarios, six in total, were considered as part of the study and reported using loading rates and recycles in the range of ~10 – 28 m/h and ~8 – 17% respectively, all initially at a temperature of 5 °C but later at upto 40°C. In addition the impact of using subnatant collector tubes and seawater are reported as are the results from three flow scenarios trialled on site at the conditions prevailing at that time. The results from the site trials were used to validate the model developed and show how close to the theoretically predicted levels were those found in practice. The modelling results themselves are presented graphically using “contours of flow velocity” and “velocity vectors”. In addition by using a combination of “vortex summing” and “vortex shedding” analysis the magnitude of vorticity, normalised by the volume, will be derived as an indication of the likely trend in turbidity that can be expected as the loading rates are increased in practice.

The results will demonstrate how the CFD modelling requires not only a degree of interpretation of the values obtained but also a need to ensure that the basis of convergence is correctly selected. Furthermore that sufficient time, a factor not previously reported by others such as Ta, C.T. et al 2001, is allowed to ensure that convergence is reached or confirmation that any instability present is “real” and possibly dynamic, repeating consistently at regular intervals.

PROJECT OUTLINE

The study was split into two parts the first a desk top study developing the CFD model from the tank dimensions schematically represented in Figure 1.0 for one of six streams forming part of a 60 Ml/d DAF plant located west of Edinburgh, Scotland and intended to supply water to the city; which at the time was progressing through its commissioning phase in advance of formally entering service. Whilst not forming part of this study a two stage flocculation stage, with each stage comprising two clockwise rotating propeller type flocculators delivering at the time of the site trial a G value of approximately 32 sec⁻¹ operating in parallel, with a total volume of 159 m³, fed each DAF stream and the subsequent collected subnatant was to be filtered through eight mono-media rapid gravity sand filters. The second part involved a full scale field trial briefly described below.

PLANT MODELLING AND BACKGROUND

The CFD modelling used was that based on a dynamic, second order, multiphase Eulerian-Eulerian Renormalisation Group k-epsilon (RNG k-ε) turbulent model, as described by Marshall et al 2002, simulating both water and air under varying conditions. The results were generated by proprietary software Ansys Fluent v.6.3.26.

Whilst the mathematical equations and their manipulation fall outside the scope of this paper the following is intended to highlight some of the mechanisms involved in the computational process. In general CFD models and calculations will utilise first principles described by the Navier-Stoke equations of mass, momentum and energy conservation. In turn the models for multiphase flows can be divided into a number of categories, however for these studies the use of the Eulerian-Eulerian model was selected as this is the most commonly used and acceptable under the conditions investigated and is based on the assumption of inter-penetrating continua. In addition it has been shown to be applicable for both continuous-continuous and continuous-dispersed systems with the latter allowing the dispersed phase to be in the form of bubbles and hence appropriate for studying DAF.

A further consideration in determining the type of model to use is the turbulence associated with any flow through the DAF cell, since in these regions there will be fluctuations in both velocity and other parameters. Therefore for the model to be representative these need to be incorporated. To achieve this there are two equations that are in general and popular use when determining the impact of transport, i.e. velocity, and hence stress in terms of Reynolds. These equations which are predominantly empirically based need to be solved for the kinetic energy of turbulence ‘k’ and the rate of dissipation of that turbulence ‘ε’.

In time and in an effort to rationalise the empirical nature of this approach the RNG Model was developed, Yakhot et al 1986. This model allowed for the effect of flows around bends or zones of recirculation rotational flow, which can be present within a standard DAF cell, to be considered.

Once the occurrence of rotational flow is recognised within the DAF cell, as reported by Amato et al 2007 and 2009, its impact on the ultimate product water quality should be considered. However, in an attempt to quantify this, the degree of rotation needs to be determined. It was concluded that this was best determined by a measure of the vorticity, where a value greater than zero indicates some degree of rotation. The more intense the degree of rotation the greater is the likely risk of disturbance of the bubble floc agglomerate and in turn an increased risk that the subnatant exiting the DAF cell will have a higher than desired turbidity.

Mathematically vorticity (ξ), a vector quantity, is defined as the curl or rot (∇) of the velocity vector (U) i.e. $\xi = \nabla \times U$. The units of vorticity are the same as the shear rate, that of s^{-1} , where a negative or positive value within a volume merely indicates that rotational direction is different or opposite.

As part of the rationale used in this paper to assess the results reference has been made to the “volume weighted average” vorticity magnitude, as given by equation (1), where ψ denotes the scalar variable of vorticity.

$$\frac{1}{V} \int \psi dV = \frac{1}{V} \sum_{i=1}^n \psi_i |V_i| \dots \dots \quad s^{-1} \quad (1)$$

METHODOLOGY

The 3D CFD model produced had a volume mesh of 4.4 million tetrahedral cells converted to 908,000 multi-faceted polyhedra, including both the flocculation cells and the flotation chamber.

It has been reported in the literature and provision in some instances has been made for a “floc-flotation transition zone”, Crossley et al 2007, to mitigate the coupling of the flow which can occur between the water leaving the flocculation stage and it entering the DAF cell, with a recommendation that consideration of this fact should be given in the design and layout of the DAF structures. The coupling can impact on the uniformity of the flow into the DAF cell, with potentially higher localised velocities promoted by the actual flocculator configuration. Whilst this has been noted these effects within the context of this paper have not been considered in any detail. The rotations of the flocculators for both the model and on site were set at clockwise. It has been assumed that whilst the lack of uniformity may alter the absolute values of any 3D results the relative values across all models from this will remain unchanged, even though the flocculator conditions changed in terms of retention time with flow. That said the flocculators were added as fixed swirl and velocity volumes derived from the tip speed, diameter and flocculator data provided by the supplier for the units installed an approach previously used by Amato et al 2007 and 2009.

The recycle nozzles and main inlet flow were set as velocity inlets. The actual nozzle arrangement in terms of the modelling was based on the plant referred to above using the actual design and including installed distribution headers and pipework. The top water surface boundary is defined as a frictionless wall. A gas sink, Ta et al 2001, was applied at the surface to remove air from the domain at a rate equal to the flux across the water surface. Gravity is a downward force across the domain. The basic recycle fraction as a proportion of the inlet flow was adjusted in accordance with that that was practically possible on site and could vary between approximately ~6 – 18% (refer to Table 4.0) whilst average spherical bubble sizes of 40 μm in the contact zone with a density equivalent to ambient air in the range 5 – 40 $^{\circ}C$ was assumed. It was further assumed that at these recycle rates, temperature and saturator pressures of 4.7 Barg that the actual dose rate of air would not result in the number of air bubbles available becoming a limiting factor in terms of floc capture and removal. The reference plant was designed to maintain a minimum air dose of 7

gm/m³ which would typically have produced at least a bubble volume concentration of ~5,500 ppm which would exceed the 3,000 ppm which Haarhoff et al 2004 reported as resulting in poor contact zone capture of floc and hence would increase the likelihood of poor product quality. In contrast floc characteristics relative to density and average spherical diameter (d_f) were assumed to be 1,010 kg/m³ and 10 – 20 μ m respectively, both values according to Haarhoff et al 2004 would maximise the capture efficiency within the contact zone.

Having established the basic bubble and floc characteristics it was necessary to consider what actually happened to these as they came into contact with each other, causing both coalescence of some bubbles and the formation of bubble floc agglomerates, assuming that no significant growth of floc occurs after the flocculation stage. Previous studies by Tambo et al 1986 have suggested that bubbles will not be attached to floc in layers and therefore the surface area available from any particular floc will in itself effectively limit the number of bubbles that can be attached. Estimates of the number of bubbles (N_b) that can be attached can be calculated by assuming that each bubble occupies a square with side dimensions equivalent to the bubble diameter (d_b).

The maximum number of bubbles that can be attached by using the above approach can be calculated using equation (2).

$$N_{\max} = \pi \left[\frac{d_f}{d_b} \right]^2 \quad (2)$$

It is clear from equation (2) that the number of bubbles that can be attached is fairly small unless further growth occurs. This fact is acknowledged by Haarhoff et al 2004 as a limitation of some of the modelling work carried out to date and therefore as such they do not accurately predict the subnatant conditions or quality. It was further stated by Haarhoff et al 2004 that for good DAF performance in terms of rise rate laminar condition needed to prevail within the DAF cell and these were linked to floc bubble agglomerates in the size range of 140 – 170 μ m. With this in mind some attempt was made within the modelling assumptions of this study to simulate both the initial formation of the agglomerate and also its growth through the contact zone and into the separation zone. It was therefore assumed that a combination of upto 50 bubbles could attach to the particles and that overall a floc bubble agglomerate with a diameter of ~148 μ m with a density in the range of 0.0015 – 0.0037 gm/cm³ would be present in the bulk of the separation zone.

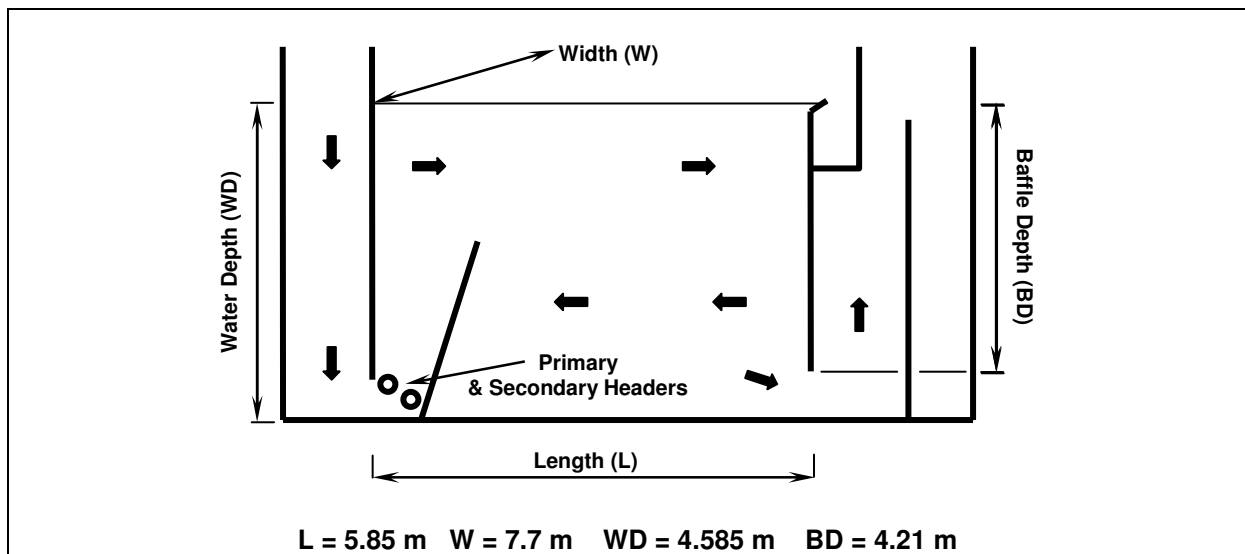
The figures above were then utilised as part of the calculations used to derive the position of the WWL. The WWL was calculated by taking the vertex average of the z-components of an isosurface of air fraction at 1×10^{-4} . The vertex or vertices here are defined as “plane tiling” with the isosurface created within the model as a “tiled floor of triangles” and therefore the vertex average is the average of the points where the triangles connect. Convergence and therefore stable conditions were assumed to have been reached when both the WWL and the total volume of air in the DAF cell, noting the losses from both the liquid surface and in the outlet subnatant flow, had reached a steady state. In the majority of the simulations run this steady state was achieved after more than 6 hours or >20,000 seconds. This approach was found to provide consistent and reliable results which were independent of the starting point.

OUTLINE PLANT AND MODEL DETAILS

Desk Top Study

The purpose here was to investigate the relationship of rate against tank depth based on certain criteria previously reported by Amato et al 2007 and 2009 regarding bubble size within the contact zone and an alternative bubble size and density to simulate the bubble floc agglomerates which form in the upper portion of the contact zone and separate in the downstream clarification or separation zone.

Figure 1.0 Tank & Model Dimensions



The change in bubble size and more importantly its density was seen as easing the computer simulations and accelerating the process without losing accuracy when not actually considering simultaneously the three phases present of water, air and solid, and is a similar approach to that reported by Guimet et al 2007. The six baseline flow scenarios and other conditions covered by the paper are summarised in Table 1.0

Table 1.0 Baseline CFD Scenarios

Scenarios	Stream Flow (m ³ /hr)	DAF Loading (m/h)	Primary Header (m ³ /hr)	Secondary Header (m ³ /hr)	Total Recycle (%)
			Using Design Nozzles etc.		
1 (Design)	443	9.84	23.572	12.693	8.19
			Assuming Temporary Trial Nozzles Installed		
2	443	9.84	46.201	30.716	17.36
3	700	15.54	46.201	30.716	10.99
4	910	20.2	46.201	30.716	8.45
5	1025	22.76	46.201	30.716	7.50
6	1261	27.99	46.201	30.716	6.10

In addition whilst not reviewed in detail two further conditions were considered. The first was to assess the internal flow dynamics within the DAF cell to determine whether any device which created minimal pressure drop or reduced apparent turbulence in itself contributed to the position of the WWL and therefore potentially the final water quality. The second was to look at the impact of typical seawater with a salinity of 35,000 mg/l at a similar temperature to the base scenarios but also at 30°C considered fairly normal for some applications in the Middle East and beyond. The intent was to show how a plant designed at a particular loading rate and tank depth might have to be modified or down rated to accommodate the different water properties between non saline and saline conditions.

Site Validation Trials

It is clear from the above that certain assumptions had to be made ahead of any field trials and therefore to validate the model and assess the accuracy or otherwise of the assumptions a small number of full scale trials were carried out. These inevitably had to be carried out under conditions that did not exactly match any of the scenarios modelled via CFD however these differences were subsequently used and the measurements of the WWL physically measured using an underwater camera and measuring rod on site were checked against those that would be predicted by the CFD model under the same conditions. In all case the camera position was fixed relative to the length and width of the DAF cell and was located centrally 2.62 m and approximately 1.0 m downstream of the inlet underflow baffle and incline baffle respectively.

Table 2.0 Raw Water Conditions

Date	pH	UV ₂₅₄ "Lab." ⁽¹⁾ Abs (cm ⁻¹)	UV ₂₅₄ "Online" ⁽¹⁾ Abs (cm ⁻¹)	Colour App. (°Hz)	Colour True (°Hz)	Turbidity (NTU)	Temp. (°C)
14/07/2009	6.20	-	-	27	21	0.46	-
15/07/2009	6.74	-	0.123	25	19	1.07	-
16/07/2009	6.14	-	0.132	32	24	0.53	-
17/07/2009	6.33	0.1165	0.106	33	28	0.306	-
23/07/2009	7.34	0.125	0.129	27	21	0.498	13.2
27/07/2009	7.84	0.15	0.143	35	28	0.696	13
29/07/2009		-	-	35	-	-	-
30/07/2009		-	-	39	-	-	-
03/08/2009	7.68	0.154	0.147	37	28	0.674	13.6
05/08/2009	7.44	0.162	0.153	36	27	0.636	13.6
06/08/2009	6.94	0.157	0.14	37	32	0.621	14.8

The site conditions prevailing at the time together with the water quality data and results are summarised in Tables 2.0 and 4.0 (a)-(b). It should be noted that at the time the plant conditions were not ideal and fully optimised and operational requirements meant that the time between flow changes and measurement were less than ideal. The reader is therefore advised that particularly with regards to the turbidity of the subnatant that this reflects that fact and should view the quality in terms of the relative differences and not in terms of achieving guarantee quality limits which were lower at 1.5 NTU as a 95%ile.

RESULTS

It should be noted that for the site trials only stream number 5 of the 6 actually available was considered and this stream was fitted with higher volumetric capacity nozzles to maintain the recycle percentages above 6% or 7 gm/m³ throughout. The saturator pressure was set and automatically regulated by the operational requirements prevailing at the time which varied between 4.9 and 5 Barg hence the slightly different recycle flows recorded to those considered in the actual modelling simulations reported. The following Tables 3.0 – 7.0 and Figures 2.0 – 8.0 summarise the results of the CFD modelling based on the Scenarios detailed in Table 1.0, using water, seawater both with and without subnatant collector tubes, the data recorded during the site trials, a rerun of a number of the of the CFD model under site conditions and also including extrapolation of the results to show graphically the location of the WWL. It should be noted that the WWL in the CFD model and reported in the following Tables was the average over the DAF cell volume, whereas those recorded during the site trial refer to a snap shot taken at a given position detailed above.

In addition an attempt was made using both the predicted and measured results obtained to calculate the likely hydraulic loading rates that could be applied assuming that the WWL would

always remain at least 250 mm, arbitrarily set, above the outlet baffle or other outlet arrangement. Therefore with reference to Figure 1.0 the target WWL was set at 3.96 m which was assumed to provide sufficient clearance between the outlet and the variable lower level of the white water, actually visually noted via the camera used, such that the risk of impacting on measured water quality leaving the DAF cell was reduced. These extrapolated results are shown in Table 6.0 and Figure 5.0.

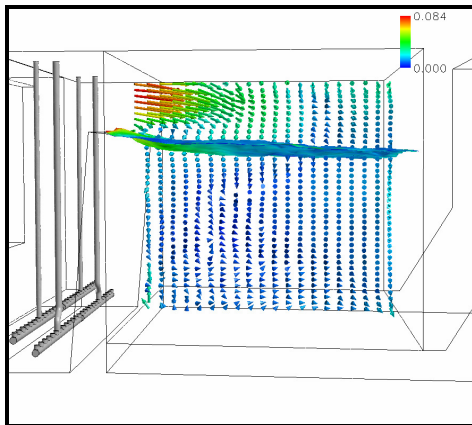
Table 3.0 Baseline CFD Results

Scenario	Inlet Flow (MI/d)	Loading Rate (m/h)	Recycle Primary Header (m ³ /hr)	Recycle Secondary Header (m ³ /hr)	Total Recycle (%)	CFD WWL		Vorticity Magnitude	
						@5 ^o C (m)	@13 ^o C (m)	@5 ^o C (s ⁻¹)	@13 ^o C (s ⁻¹)
1	10.6	9.84	23.6	12.7	8.2	1.44	1.33	0.106	0.110
2	10.6	9.84	46.2	30.7	17.4	1.61	1.37	0.138	0.140
3	16.8	15.54	46.2	30.7	11.0	3.53	2.44	0.137	0.140
4	21.8	20.2	46.2	30.7	8.5	4.34 [†]	3.39	0.132	0.137
5	24.6	22.76	46.2	30.7	7.5	4.34 [†]	4.06	0.153	0.143
6	30.3	27.99	46.2	30.7	6.1	4.34 [†]	4.34 [†]	0.170	0.166

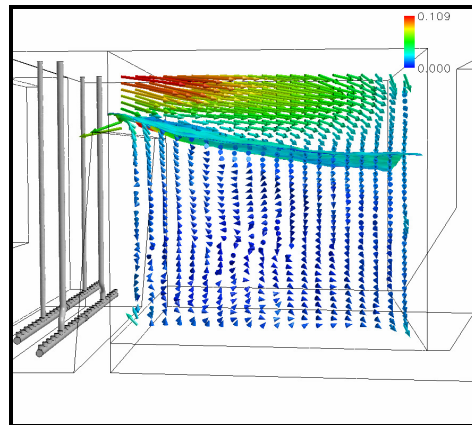
Note Above and in following Tables † indicate that the WWL is below the outlet baffle.

Figure 2.0 CFD Plots For Baseline CFD Scenarios

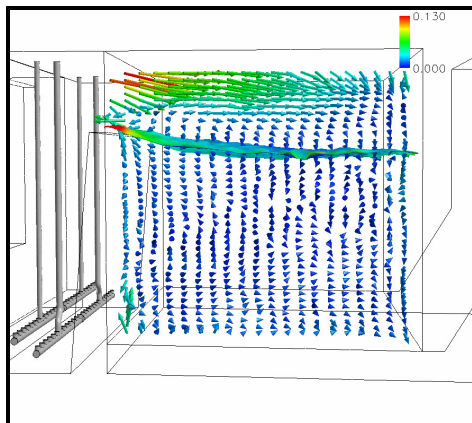
(a) 10.6 MI/d (Design), 9.84 m/h
~8% Recycle & 13^oC



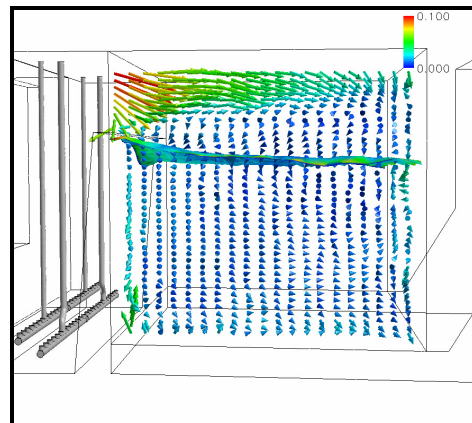
(b) 10.6 MI/d (Design), 9.84 m/h
~8% Recycle & 5^oC



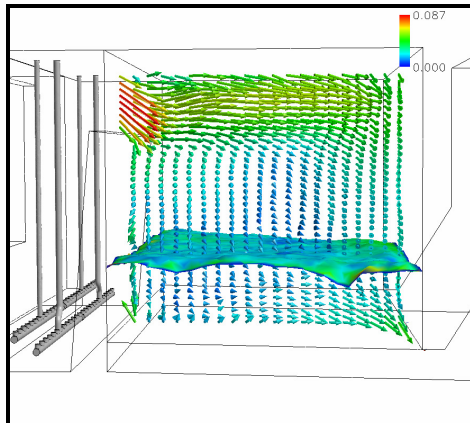
(c) 10.6 MI/d, 9.84 m/h
~17% Recycle & 13^oC



(d) 10.6 MI/d, 9.84 m/h
~17% Recycle & 5^oC



(e) 21.8 MI/d, 20.2 m/h
~8.5% Recycle & 13°C



(f) 21.8 MI/d, 20.2 m/h
~8.5% Recycle & 5°C

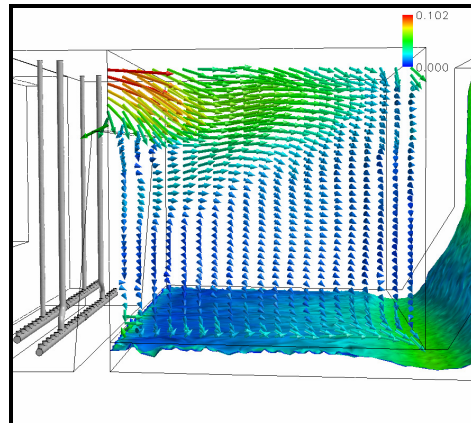


Table 4.0(a) Site Measurements: Inlet Conditions To DAF Cells

Plant Flow (MI/d)	Streams in service	Stream No.	Flow/Stream & Flocculator Retention		Sat. Pressure (Barg)	Recycle Headers Primary (m ³ /hr)	Recycle Header Secondary (m ³ /hr)	Total Recycle (m ³ /hr)	Recycle (%)
			(MI/d)	(min)					
10.2	1	5	10.2	22.5	4.9	46.93	31.20	78.13	18.38
30	4	5	7.5	30.5	5	47.40	0	47.40	15.17
30	3	5	10	22.9	5	47.40	0	47.40	11.38
-	-	2	10	22.9	5	23.94	13.02	36.96	8.87
-	-	3	10	22.9	5	23.94	13.02	36.96	8.87
30	1	5	30	7.6	5	47.40	31.51	78.91	6.31
30	2	5	15	15.3	5	47.40	31.51	78.91	12.63

Table 4.0(b) Site Measurements: DAF Cell Subnatant Conditions

Site Trial No.	Temp. (°C)	DAF Cell Loading (m/h)	Turbidity (NTU)	Unfiltered UV ₂₅₄ "Lab." ⁽¹⁾ Abs (cm ⁻¹)	Filtered UV ₂₅₄ "Lab." ⁽¹⁾ Abs (cm ⁻¹)	Al. Total mg Al/l	Al. Soluble mg Al/l	Dose mg Al/l ⁽²⁾	WWL Depth (m)
1	13.2	9.4	N/D	-	-	-	-	-	1.45
2	13.8	6.9	1.26	0.065	0.0175	0.55	0.049	2	N/D
3(a)	13.8	9.3	1.37	0.072	0.018	0.57	0.045	2	1.45
3(b)	13.8	9.3	2.53	0.11	N/D	0.79	N/D	2	N/D
3(c)	13.8	9.3	1.86	0.096	N/D	0.65	N/D	2	N/D
4	13.8	27.8	3.08	0.116	0.0245	1.24	0.035	2	4.435
5	13.8	13.9	1.79	0.092	0.019	0.77	0.049	2	2.475

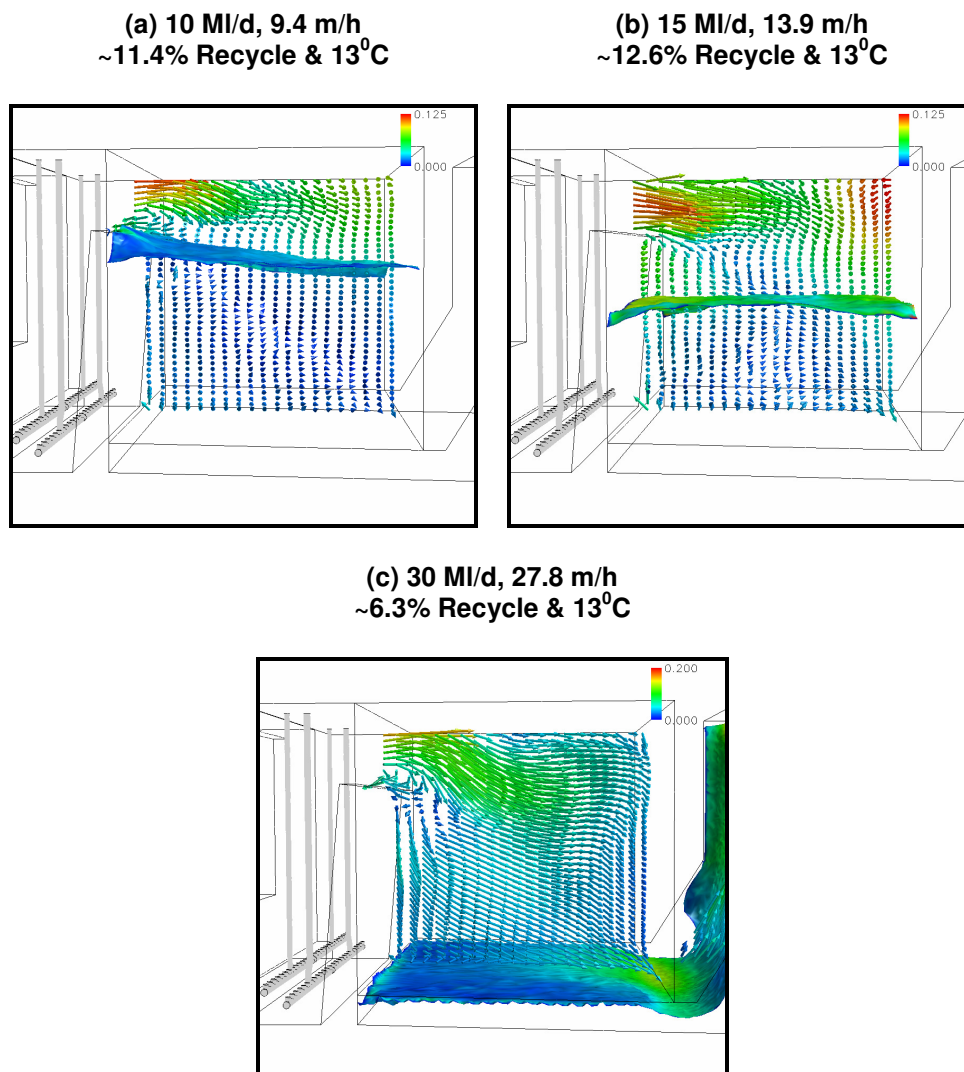
- Note (1) "Lab", indicates sample measured in the laboratory, whilst "online" refers to the meter installed in the field.
 (2) Coagulation pH under these conditions were measure in the common dosed inlet channel at 5.6, whilst jar tests had suggested an ideal pH of ~6.2 for the most efficient operation of the DAF in terms of water clarity.

With reference to the site results summarised in Tables 4.0 (a) and (b) the following CFD plots were produced using the water temperature recorded at the time of ~ 13°C and then comparing these results with an assumed raw water temperature of 5°C as summarised in Table 5.0.

Table 5.0 CFD Simulations Based On Site Conditions Of Temperature And Flow And Comparing With An Assumed Temperature Of 5°C

Scenario	Inlet Flow (MI/d)	Temp. (°C)	Recycle Headers Primary (m ³ /hr)	Recycle Header Secondary (m ³ /hr)	Total Recycle (%)	CFD WWL (m)	Site WWL (m)	Vorticity Magnitude (s ⁻¹)
1	10	13	47.4	0	11.4	1.52	1.45	0.121
2	15	13	47.4	30.15	12.6	2.52	2.48	0.141
3	30	13	47.4	30.15	6.3	4.34 [†]	4.44 [†]	0.155
4	10	5	47.4	0	11.4	1.84	-	0.118
5	15	5	47.4	30.15	12.6	3.20	-	0.137
6	30	5	47.4	30.15	6.3	4.34 [†]	-	0.165

Figure 3.0 CFD Vector Plots Based On Site Trial Conditions



Noting the close correlation between predicted and site measured WWL as evident from Table 5.0 Scenarios 5(1) – 5(3) it was assumed that the predicted WWL at the temperatures modelled could be plotted and relationships developed. Therefore with reference to Figure 4.0 and the linear curve fitting equations derived it can be calculated that at 5°C and 13°C assuming a lower WWL level of 3.96 m that the maximum flow rate that could be applied would be ~18 MI/d and ~24.5 MI/d respectively which would equate to a net hydraulic loading rate of 16.7 m/h and 22.7 m/h respectively. (Refer to Figure 7.0 for an example of the CFD vector plot at 16.7 m/h.) If the figures

are further extrapolated as shown graphically in Figure 5.0 then possible rates achievable at say 20°C and 40°C can be derived, whilst still maintaining the target WWL of 3.96m referred to above, as ~30.3 MI/d and ~46 MI/d respectively, which in turn would equate to a net hydraulic loading rate of 27.8 m/h and 42.6 m/h respectively.

Figure 4.0 CFD Predicted v Measured WWL Values

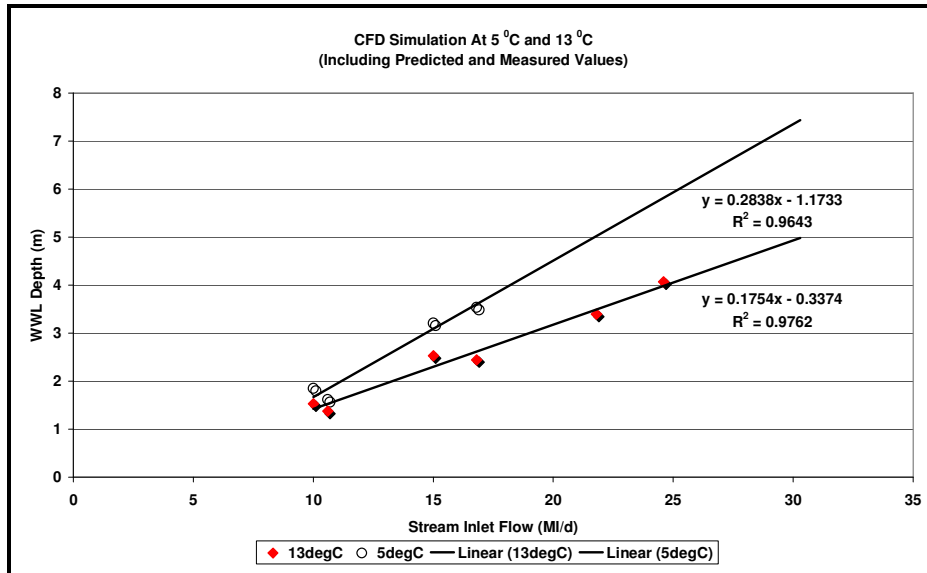


Figure 5.0 CFD Predicted Rate v Temperature

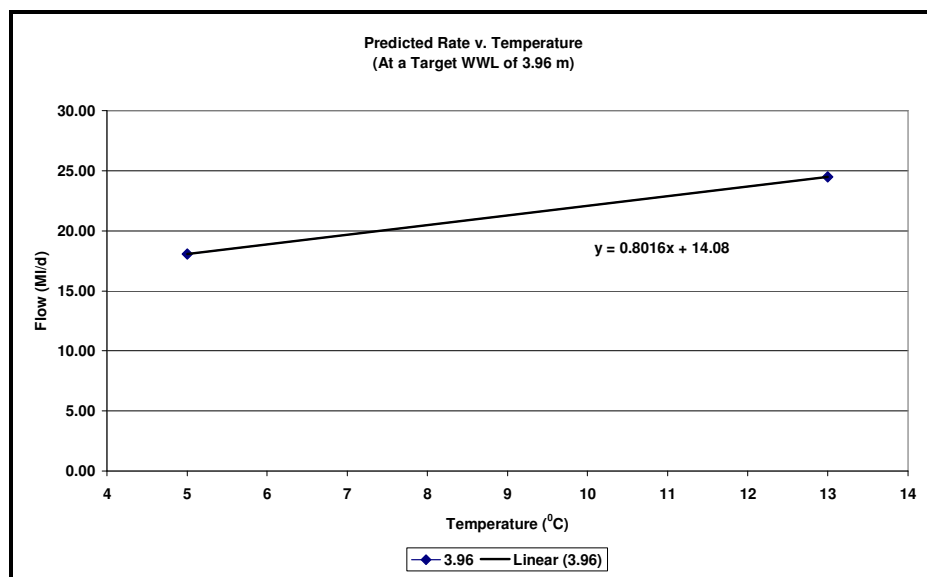


Table 6.0 Original CFD Scenarios (Table 1.0) Run Under Site Temperature Conditions.

Scenario	Inlet Flow (MI/d)	Temp. (°C)	Recycle Primary Header (m³/hr)	Recycle Secondary Header (m³/hr)	Total Recycle (%)	CFD WWL (m)	Vorticity Magnitude (s⁻¹)
1	10.6	13	23.6	12.7	8.2	1.33	0.110
2	10.6	13	46.2	30.7	17.4	1.37	0.140
3	16.8	13	46.2	30.7	11.0	2.44	0.140
4	21.8	13	46.2	30.7	8.5	3.39	0.137
5	24.6	13	46.2	30.7	7.5	4.06	0.143
6	30.3	13	46.2	30.7	6.1	4.34 [†]	0.166

When these derived figures are actually used with the CFD model then the predicted WWL is within 150-320 mm off the bottom of the outlet baffle, these results are summarised in Table 7.0 as results 7(1) to 7(4). These rates were further assessed using subnatant or collector tubes to see if the model predicted any difference to the final WWL, these results are summarised as part of Table 8.0. In both cases one or more of the scenarios in Tables 7.0 and 8.0 were run under seawater conditions.

It should be noted that the basis for sizing the orifices located on the invert of the subnatant tubes was based on three simple conditions, these were that the total free area provided was equal to, less than or greater than the total free area provided in this model by the outlet underflow baffle. The extent of the differences was arbitrarily set at $\sim\pm 10\%$. These three arrangements were simulated and it was noted that provided the total free area of the orifices was equal to or greater than the free area provided by the outlet under flow baffle then the CFD predicted that if tubes were installed then they would result in a WWL equal to or slightly above that seen at the same rate and temperature without them. However in all cases where the free area was less than that provided by the outlet underflow baffle then the WWL would be lower under all conditions meaning that lower rates would have to be applied than if the tubes had not been installed. A further point to note is that when reporting the WWL with the tubes installed that since the computer calculations actually includes any air around the orifices or tubes, which in turn can result in lower WWL than is actually the case, an estimate of the WWL off the graphics package had to be made. In light of this the accuracy of the WWL with tubes should be regarded as $\pm 0.1\text{m}$. In contrast when referring to the same runs without tubes it is noticeable that the CFD model shows a WWL that dips towards the outlet, as evident from Figures 7.0 and 8.0, this is likely to have skewed the levels and resulting in lower values being reported than might be the case in practice. A summary of the results are reported here by way of example as part of Table 8.0.

When considering the impact of the highest rate predicted of $\sim 46\text{ MI/d}$ both in terms of water and seawater it will be noted from Tables 7.0 and 8.0 that the recycle rate falls below the industry minimum norm of 6% and as was reported by [Lundh et al 2001](#) the flow structures under these conditions can become unstable. If this was actually to be trialled on site then it's highly probable that the subnatant quality from the DAF would be compromised at the temperature simulated at equivalent loading rate of 42.6 m/h and possibly even for the lower loading rate of 27.8 m/h.

Table 7.0 CFD Results Based On Predicted Flows, Water And Seawater

Scenario	Inlet Flow	Temp.	Recycle Headers Primary	Recycle Header Secondary	Total Recycle	CFD WWL	Vorticity Magnitude
	(MI/d)	(°C)	(m ³ /hr)	(m ³ /hr)	(%)	(m)	(s ⁻¹)
1	18	5	46.2	30.7	10.25	3.89	0.148
2	30.3	20	46.2	30.7	6.1	4.05	0.149
3	30.3	30	46.2	30.7	6.1	3.83	0.160
4	46	40	46.2	30.7	4.0	4.06	0.189
1sw	18	5	46.2	30.7	10.25	4.34 [†]	-
2sw	30.3	20	46.2	30.7	6.1	4.34 [†]	-
4sw	30.3	30	46.2	30.7	6.1	3.90	0.163
3sw	46	40	46.2	30.7	4.0	4.34 [†]	-

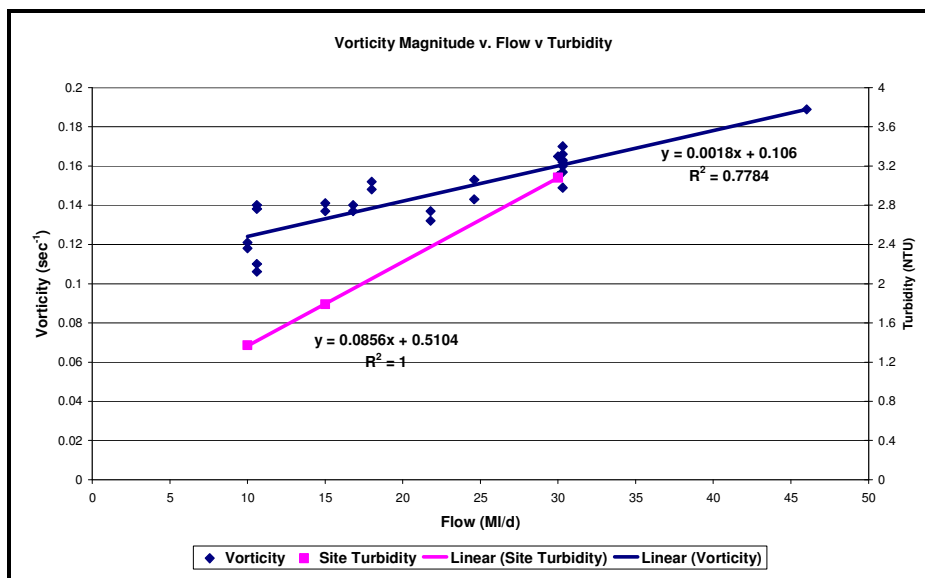
Whilst this fact was noted it was decided to carryout further simulations where the recycle rate was maintained at $\sim 6\%$, though one run was carried out at 12% recycle with subnatant tubes, this did not appear to provide any obvious benefit and for this exercise no further runs were completed. Therefore the 6% recycle rate was selected for consistency between water and seawater simulations. It however should be recognised that certainly when treating seawater, which formed part of this study, that due to the salting out effect reported by Masterton 1975 which will reduce the amount of air that is available for precipitation per unit volume of recycle then higher rates may

very well be required for certain applications which in turn may impact on the final WWL found in practice.

In addition to the selected recycle rate a temperature of 30°C was set for the seawater. The seawater temperature selected was based on the author's recent experience which suggested that the use of DAF as a pre-treatment stage ahead of membrane systems in the Middle East and other arid and warm regions around the World was gaining popularity and therefore appropriate here for consideration.

If all the vorticity magnitude values calculated are plotted and related to the turbidity measured on site whilst the results are fairly limited it can be seen as previously reported by Amato et al 2007 and 2009 that as flow increase so does the vorticity and in turn so does the turbidity. This simple relationship can be seen from Figure 6.0.

Figure 6.0 Vorticity Magnitude, Flow And Turbidity



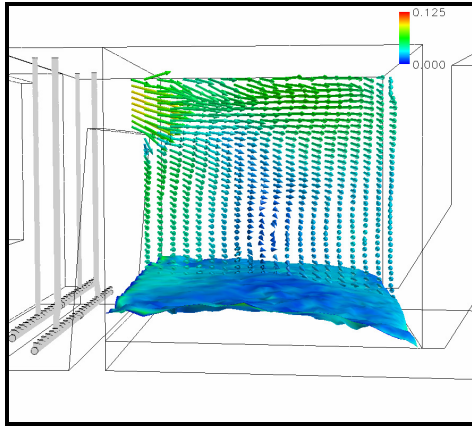
In addition if the relative increase in flow and vorticity is compared over the same range then from Figure 6.0 it can be deduced that with a 3x increase in flow from 10 to 30 MI/d the vorticity increased from ~0.12 sec⁻¹ to ~0.16 sec⁻¹, an increase of 1.33x. If then these ratios of flow and vorticity are compared a further ratio of ~2.26:1 can be derived. Then noting that the initial turbidity measured on site at 10 MI/d was recorded at 1.37 NTU if this is multiplied by the ratio figure derived here this would predict a final turbidity of 3.10 NTU, the actual value was 3.08 NTU.

Table 8.0 CFD Subnatant Tube Scenarios

Scenario	Inlet Flow (MI/d)	Temp. (°C)	Recycle Primary Header (m ³ /hr)	Recycle Secondary Header (m ³ /hr)	Total Recycle (%)	CFD WWL (m)	Vorticity Magnitude (s ⁻¹)
1s	18	5	46.2	30.7	10.3	3.05	0.152
2s	30.3	20	46.2	30.7	6.1	4.34 [†]	-
3s	30.3	30	90	60	12	4.34 [†]	-
4s	30.3	30	46.2	30.7	6.1	3.17	0.162
5s (seawater)	30.3	30	46.2	30.7	6.1	3.40	0.157
6s	46	40	46.2	30.7	4	4.34 [†]	-

Figure 7.0 CFD Predicted WWL And Vector Plot At 5°C With And Without Subnatant Tubes

**(a) 18 MI/d, 16.7 m/h
Without Subnatant Tubes
~10.3% Recycle & 5°C**



**(b) 18 MI/d, 16.7 m/h
With Subnatant Tubes
~10.3% Recycle & 5°C**

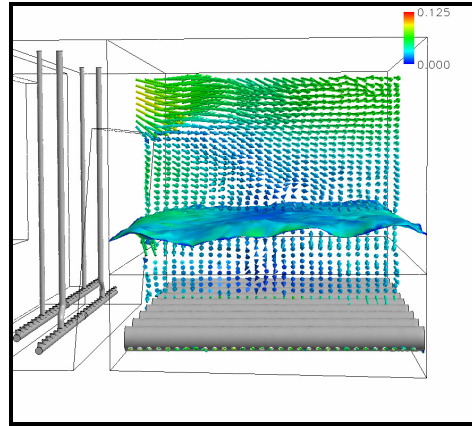
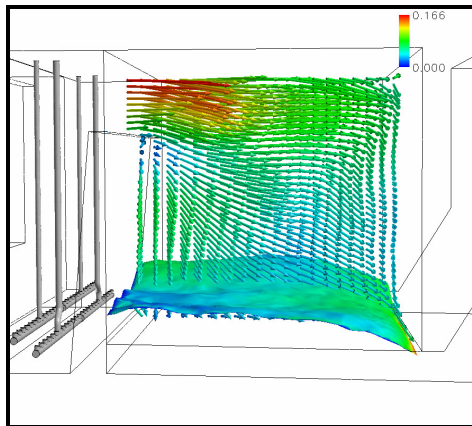
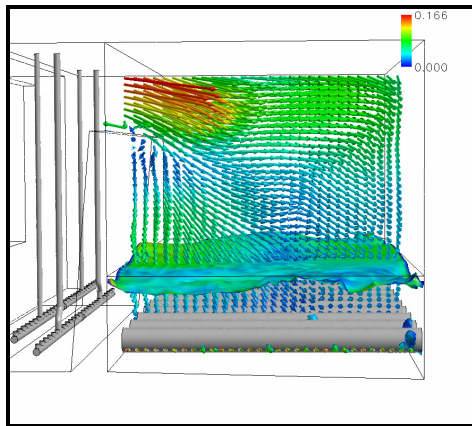


Figure 8.0 CFD Predicted WWL And Vector Plot For Water And Seawater With And Without Subnatant Tubes

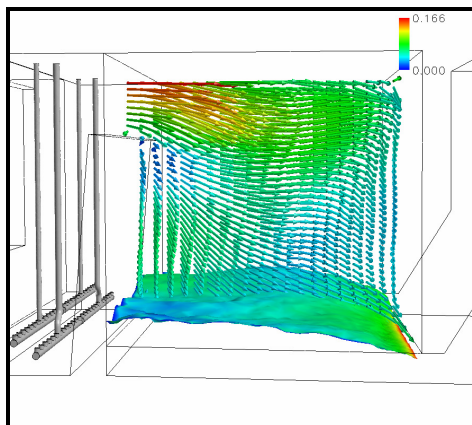
**(a) 30.3 MI/d, 28 m/h
Without Subnatant Tubes
~6.1% Recycle & 30°C**



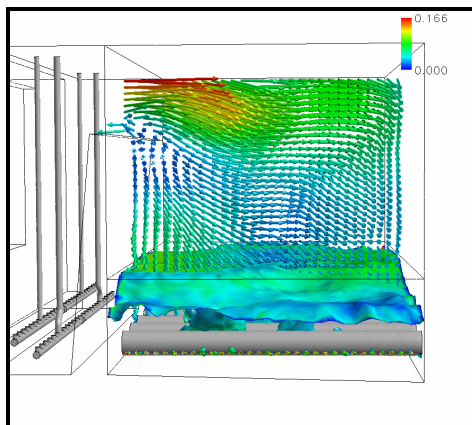
**(b) 30.3 MI/d, 28 m/h @
With Subnatant Tubes
~6.1% Recycle & 30°C**



**(c) 30.3 MI/d, 28 m/h
Seawater Without Subnatant Tubes
~6.1% Recycle & 30°C**



**(d) 30.3 MI/d, 28 m/h
Seawater With Subnatant Tubes
~6.1% Recycle & 30°C**



CONCLUSIONS

It can clearly be seen from the results reported both from the CFD desk top study and the field trials that the final turbidity and therefore water quality from the DAF, assuming appropriate chemical pre-treatment is applied, is not only a function of loading rate but tank depth.

The relationship first reported by Amato et al 2007 and [2009](#), that of increasing vorticity magnitude will result in an increasing level of DAF subnatant turbidity has again been shown to be true, on this occasion for a variety of conditions such as temperature and water type. The evidence compiled also suggests that both parameters are linked to the position of the WWL which should in any good DAF design always be retained within the confines of the DAF cell. Though it should be noted failure to do so will not necessarily always result in poor water quality, though clearly the risk of this being the case will increase significantly.

The impact of lower temperatures in driving the WWL down if all other conditions remain the same can be partially mitigated by increasing the recycle as evident from Figure 2.0(b) and 2.0(d). That said as the recycle is increased so will the depth of the WWL and therefore should the recycle be increased when the WWL is already low in the tank, then adding more, may simply push it down further to a point where it will start to leave the cell making the lower portion of the stratified white water unstable.

The predicted and actual WWL measured on site, albeit for a relatively small number of full scale trials, demonstrate that the assumptions made to date within the model are appropriate and with more trialling their robustness can be confirmed. It can therefore be concluded that in the absence of further data the present model can be used as a predictive tool in assessing the relative tank depth that should be provided given the water temperature and loading rate to be applied. Furthermore in the case of seawater the WWL predicted can be assumed to be upto ~200mm lower than would be the case under the same conditions treating a non saline source.

The use of subnatant collection tubes and it's assumed to be true for other similar "distribution" devices located in the bottom of a DAF cell, appear to only provide marginal benefits in terms of reducing the depth of tank that could be provided. The potential savings would appear to be up to ~500 mm of tank depth and this at the lower temperatures, as evident from Figures 7(b) and 8(b). However there is no evidence that there would be any significant increased security in terms of achieving the desired water quality. Clearly the designer would need to assess the cost benefits of such provision in terms of the one off cost of providing a slightly deeper tank over the cost of the tubes or similar, together with the additional maintenance that such a system requires by way of access. Furthermore the hydraulic design of such systems which may utilise headloss to ensure distribution, will need to take due cognisance of the apparent affect referred to earlier when the free area provided by the orifices within the subnatant tubes was less than that available with a simple underflow outlet baffle; such systems may result in the WWL being lower than desirable and therefore putting the subnatant water quality at risk.

It is clear that there is still further work required to fully substantiate some of the findings reported, but that said there is sufficient evidence to show that the primary objective of this study, that of deriving a predictive tool relating rate, tank depth to a likelihood of achieving the desired water quality were achieved with the aid of CFD.

ACKNOWLEDGEMENTS

The authors would like to acknowledge the support of Scottish Water and assistance provided by the site and staff, in particular Ed Irvine and Findlay Donaldson, in making it possible for the site trials to be completed during a particularly busy period.

REFERENCES

Amato, T., Wicks, J. 2007 The Practical Application Of Computational Fluid Dynamics To Dissolved Air Flotation, Water Treatment Plant Operation, Design And Development. *Proc Flotation 2007, 5th International Conference on Flotation in Water & Wastewater Systems, Seoul, September, 105-112*

Amato, T., Wicks, J. 2009 The Practical Application Of Computational Fluid Dynamics To Dissolved Air Flotation, Water Treatment Plant Operation, Design And Development. *J. Wat. Sup. Res. & Technol.-AQUA. 58.1, 65-73*

Guimet, V., Broutin, P., Vion, P. & Glucina, K. 2007 *Proc Flotation 2007, 5th International Conference on Flotation in Water & Wastewater Systems, Seoul, September, 113-119*

Ta, C.T., Beckley, J. & Eades, A. 2001 A Multiphase CFD Model Of DAF Process. *Wat. Sci. Technol. 43(8), 153-157*

Marshall, E.M. & Bakker, A. 2002 Computational Fluid Mixing. *Fluent Inc. Lebanon (USA)*

Yakhot, V. & Orszag, S.A. (1986) Renormalisation Group Analysis of turbulence:1 Basic Theory. *Journal of Scientific Computing 1(1), p1-51*

Crossley, I.A., Herzner, J., Bishop, S.L., & Smith, P.D. Going Underground – Constructing New York City's First Water Treatment Plant, A 1,100 Ml/d Dissolved Air Flotation, Filtration And UV Facility *Proc Flotation 2007, 5th International Conference on Flotation in Water & Wastewater Systems, Seoul, September, 143-151*

Haarhoff, J. & Edzwald, J.K. 2004 Dissolved Air Flotation Modelling: Insight And Shortcomings *J. Wat. Sup. Res. & Technol.-AQUA. 53.3, 127-150*

Tambo, N., Matsui, Y. & Fukushi, K. 1986 A Kinetic Study of Dissolved Air Flotation. *World Congress of Chemical Engineering, Tokyo*

Lundh, M., Jönsson, L and Dahlquist, J. 2001 The Flow Structure In The Separation Zone Of A DAF Pilot Plant And The Relation With Bubble Concentration. *Wat. Sci. Technol. 43(8), 185-194*

Masterton, W.L. 1975 Salting Coefficients for Gases in Seawater from Scaled Particle Theory. *J Solution Chemistry Vol. 4(6), 523-534*